Non-monotonic confining potential for generalized random matrix model

Swapnil Yadav[1], Kazi Alam[1], K. A. Muttalib[1] and Dong Wang[2]

[1]*Department of Physics, University of Florida, Gainesville, FL 32611-8440, USA*
[2]*Department of Mathematics, National University of Singapore, Singapore*
(Dated: October 22, 2020)

We consider a limiting case of the joint probability distribution for a random matrix ensemble with an additional interaction term controlled by an exponent γ (called the γ-ensembles), which is equivalent to the probability distribution of Laguerre β-ensembles. The effective potential, which is essentially the confining potential for an equivalent ensemble with $\gamma = 1$ (called the Muttalib-Borodin ensemble), is a crucial quantity defined in solution to the Riemann-Hilbert problem associated with the γ-ensembles. It enables us to numerically compute the eigenvalue density of Laguerre β-ensembles for all $\beta > 1$. In addition, the effective potential shows a non-monotonic behavior for $\gamma < 1$, suggestive of its possible role in developing a transition from a diverging to a non-diverging density near the hard-edge of the eigenvalue spectrum. Such a transition in eigenvalue density is of critical importance for the random matrix theory describing disordered mesoscopic systems. For γ-ensembles with $\gamma > 1$, the effective potential also shows transition from non-monotonic to monotonic behavior near the origin when a parameter of the additional interaction term is varied.

I. INTRODUCTION

A generalized random matrix model with additional interactions [1], called the γ-ensembles, was introduced recently as a solvable toy model for three-dimensional (3D) disordered conductors. The joint probability distribution (jpd) of the N non-negative eigenvalues x_i for these γ-ensembles has the form

$$p(\{x_i\}; \theta, \gamma) \propto \prod_{i=1}^{N} w(x_i) \prod_{i<j} |x_i - x_j| |x_i^\theta - x_j^\theta|^\gamma, \quad (1.1)$$

$$0 < \gamma, \quad 1 < \theta < \infty.$$

Here we assume the convention $w(x) = e^{-NV(x)}$, so that the empirical distribution of the particles (a.k.a. the equilibrium measure) converges as $N \to \infty$. In [1], the parameter γ was restricted to $0 < \gamma \le 1$, but the method developed there allows the evaluation of the density of eigenvalues of the γ-ensembles for any $\gamma > 0$, $\theta > 1$ and for any well behaved $V(x)$. In particular, it was shown that the jpd for the γ-ensembles can be mapped on to the Muttalib-Borodin ensembles [2–6] (which has the same jpd as (1.1), with $\gamma = 1$), by replacing the external potential $V(x)$ with a γ-dependent effective potential $V_{\text{eff}}(x; \gamma)$. This effective potential was calculated explicitly for $\theta = 2$ by numerically solving the Riemann-Hilbert (RH) problem associated with the jpd of the γ-ensembles.

In this paper, we first consider the limit $\theta \to 1$ and $V(x) = 2x$. We will be interested in two sets of values for the exponent γ, namely, $\gamma < 1$ and $\gamma > 1$. Following the numerical solution to the RH problem of γ-ensembles explained in [1], we first compute the effective potentials and then the corresponding eigenvalue densities for these different values of γ. The effective potentials for different γ show an interesting behavior. Near the origin, effective potentials for $\gamma > 1$ are monotonically increasing, while those for $\gamma < 1$ become non-monotonic, initially decreasing with increasing x. The minimum of the effective potential moves further away from the origin as γ is

systematically decreased from 1. Such a non-monotonic potential has been shown [7] to give rise to a 'hard-edge to soft-edge' transition in density, i.e., a transition from a density diverging near the hard edge at the origin to a density going to zero at a soft edge near the origin. This type of transition is of keen interest for transport problem in mesoscopic systems as it can describe disorder-induced metal to insulator transition in 3D disordered conductors, where only small $x_i \ll 1$ contributes significantly to the conductance [8].

It has been argued that in contrast to a quasi 1D system considered in [2], describing a 3D disordered conductor requires a disorder-dependent parameter γ that controls the strength of the additional two-body interaction [9–12]. The exponent γ decreases from 1 as the strength of disorder increases. The jpd describing a 3D disordered system has been proposed to be of the general form [12]

$$p(\{x_i\}; \gamma) \propto \prod_{i=1}^{N} w(x_i, \gamma) \prod_{i<j} |x_i - x_j| |s(x_i) - s(x_j)|^\gamma, \quad (1.2)$$

where $s(x) = \sinh^2 \sqrt{x}$, and the potential $V(x, \gamma)$ has a dominant linear dependence on x in the strongly disordered regime, whose strength depends on the parameter γ. The γ-ensemble defined by (1.1) was proposed as a solvable toy model replacing (1.2), which allows one to explore and study the role of the parameter γ. An eigenvalue density diverging near the origin implies the presence of a large number of small eigenvalues x_i, and hence, describes a metal with large conductance g. In contrast, a non-divergent eigenvalue density with a soft edge away from the origin describes an insulator with exponentially small conductance. However, the γ-ensemble with $\theta = 2$ studied in detail in [1] did not show any hint of such a transition in the density as γ was decreased systematically from 1.

In this work we show that for γ-ensembles defined by (1.1) with θ close to 1, the effective potential does indeed

develop a clear non-monotonicity as γ is reduced from greater than 1 to less than 1. While this change in the effective potential is still not large enough to produce a transition in density, the change is suggestive of role of disorder dependent parameter γ in realizing a transition from a diverging to a non-diverging density near the hard-edge in a more realistic model given, for example, by equation (1.2). We also observe that the effective potential develops non-monotonic behavior even in case of $\gamma > 1$ for parameter $\theta > 1$ and then gradually changes to monotonic behavior as $\theta \to 1$. As a bonus, since the $\theta \to 1$ limit is equivalent to a Laguerre β-ensemble, the model allows us to compute the eigenvalue density of Laguerre β-ensembles. These ensembles are characterized by the jpd

$$p(\{x_i\}) \propto \prod_{i=1}^{N} w(x_i) \prod_{i<j} |x_i - x_j|^{\beta},$$
$$w(x) = e^{-\frac{\beta}{2}x} \text{ or } w(x) = e^{-N\frac{\beta}{2}x}, \quad \beta > 1. \tag{1.3}$$

The limiting eigenvalue density of Laguerre β-ensembles for $\beta = 1, 2$ and 4 is known analytically [13] and is given as,

$$\sigma(x) = \begin{cases} \frac{1}{2\pi}\left(\frac{4-x}{x}\right)^{\frac{1}{2}}, & \text{for } 0 < x < 4, \\ 0, & \text{for } x \geq 4. \end{cases} \tag{1.4}$$

Later it was shown [14, 15] that the above equation is also true for all values of β. With the limit $\theta \to 1$, $V(x) = \frac{\beta}{2}x$ and $\gamma = \beta - 1$, the γ-ensemble jpd in equation (1.1) approaches jpd for Laguerre β-ensembles defined in equation (1.3). Thus with these limits for θ and γ along with appropriate $V(x)$, we can numerically compute eigenvalue density of β-ensembles for any $\beta > 1$. For Laguerre β-ensembles at $\beta = 4$, we choose $\gamma = 3$ and $V(x) = 2x$. Our numerical result for eigenvalue density shows excellent agreement with the analytical result (1.4), except very close to the soft edge. Next we systematically vary exponent $\gamma(= \beta - 1)$, keeping the external potential ($V(x) = 2x$) the same. The eigenvalue densities thus obtained, after appropriate scaling, lie on top of each other and are equivalent to eigenvalue densities of Laguerre β-ensemble in equation (1.4). All the densities diverge near hard edge with the exponent $-\frac{1}{2}$. The parameters of the fit for the density near origin also show an excellent agreement with the analytical expressions. The overall agreements with known and expected results verify that the effective potential method developed in [1] is a powerful tool that can be used for all $\gamma > 0$.

The paper is organized as follows. In Section II we give some details of the numerical solution to RH problem for γ ensembles. The equilibrium density can be obtained replacing external potential $V(x)$ with γ dependent effective potential $V_{\text{eff}}(x; \gamma)$. In Section III we obtain jpd for β ensembles as limiting case of jpd for γ ensembles and show how to compute eigenvalue density numerically for any $\beta > 1$. In Section IV we compute effective potentials and equilibrium densities by systematically varying

exponent γ, keeping the external potential $V(x) = 2x$. We also show the results for equilibrium density of Laguerre β ensembles at $\beta = 4$ and compare it with known analytical result. Finally, we analytically solve the RH problem for $\theta = 1$ to find the exact expressions of effective potentials for Laguerre β ensembles and show that they are consistent with our $\theta \to 1$ numerical results.

II. THE EQUILIBRIUM PROBLEM FOR γ ENSEMBLE

Here we give a brief overview of the solution to the RH problem of γ-ensembles and the computation of its eigenvalue density. The complete analysis can be found in [1]. Consider the γ-ensembles defined by the jpd in equation (1.1). The unique equilibrium measure μ that minimizes the energy functional

$$\frac{1}{2}\iint \ln\frac{1}{|x-y|}d\mu(x)d\mu(y) + \frac{\gamma}{2}\iint \ln\frac{1}{|x^\theta - y^\theta|}d\mu(x)d\mu(y)$$
$$+ \int V(x)d\mu(x), \tag{2.1}$$

satisfies the Euler-Lagrange (EL) equation

$$\int \ln|x-y|d\mu(y) + \gamma\int \ln|x^\theta - y^\theta|d\mu(y) - V(x) = \ell \tag{2.2}$$

if x lies inside the support of density and the equality sign is replaced by $<$ if x lies outside the support. Here ℓ is some constant. In formulating the RH problem from the above EL equations, crucial role is played by the Joukowsky Transformation (JT) for hard edge,

$$J_c(s) = c(s+1)\left(\frac{s+1}{s}\right)^{\frac{1}{\theta}}, \tag{2.3}$$

where s is a complex variable. The points in the complex domain, which are mapped by the JT on to a real line, form a contour ν given by,

$$r(\phi) = \tan\left(\frac{\phi}{1+\theta}\right)\Big/\left[\sin\phi - \cos\phi\tan\left(\frac{\phi}{1+\theta}\right)\right], \tag{2.4}$$

where $0 < \phi < 2\pi$ is the argument of s in the complex plane. Schematic Figure 1 shows mapping of all points on contour ν to two different regions in the complex plane by the JT $J_c(s)$. By defining complex transforms

$$g(z) \equiv \int \log(z - x)d\mu(x), \qquad z \in \mathbb{C}\backslash(-\infty, b],$$
$$\tilde{g}(z) \equiv \int \log(z^\theta - x^\theta)d\mu(x), \quad z \in \mathbb{H}_\theta\backslash(0, b], \tag{2.5}$$

with their derivatives $G(s) \equiv g'(s)$, $\tilde{G}(s) \equiv \tilde{g}'(s)$ and the function $M(s)$ as,

$$M(s) \equiv \begin{cases} G(J_c(s)), & \text{for } s \in \mathbb{C}\backslash\bar{D}, \\ \tilde{G}(J_c(s)), & \text{for } s \in D\backslash[-1, 0], \end{cases} \tag{2.6}$$
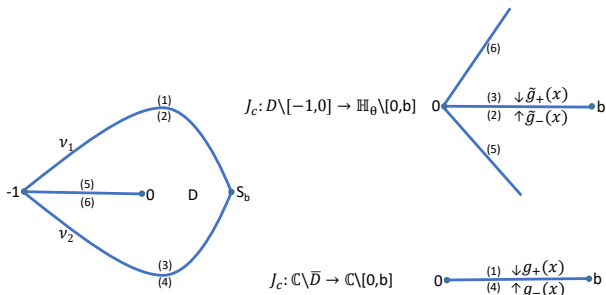
FIG. 1: (Color online) Schematic figure for the mapping of JT

the sum and difference of the EL equations can be written as

$$M_+(s_1) + \gamma M_-(s_1) + M_-(s_2) + \gamma M_+(s_2) = 2V'(J_c(s)),$$
$$M_+(s_1) - M_-(s_2) + M_-(s_1) - M_+(s_2) = 0. \tag{2.7}$$

Here $s_1 \in \nu_1$ and $s_2 \in \nu_2$ (see Figure 1). Equation (2.7), together with some of the limits of $M(s)$, form the RH problem for $M(s)$. The RH problem in terms of $N(s) \equiv M(s)J_c(s)$ is then

RH problem for N:

- N is analytic in $\mathbb{C} \setminus \nu$.

- $N_+(s_1) + \gamma N_-(s_1) + N_-(s_2) + \gamma N_+(s_2)$
  $= 2V'(J_c(s))J_c(s)$

  $$N_+(s_1) - N_-(s_2) + N_-(s_1) - N_+(s_2) = 0. \tag{2.8}$$

- $N(0) = \theta$ and $N(s) \to 1$ as $s \to \infty$.

We further define a function f such that,

$$f(J_c(s)) \equiv N_+(s) + N_-(s). \tag{2.9}$$

This gives solution to RH problem of $N(s)$ as,

$$N(s) = \begin{cases} \frac{-1}{2\pi i} \oint_\nu \frac{f(J_c(\xi))}{\xi - s} d\xi + 1, & s \in \mathbb{C} \setminus \bar{D}, \\ \frac{1}{2\pi i} \oint_\nu \frac{f(J_c(\xi))}{\xi - s} d\xi - 1, & s \in D \setminus [-1,0]. \end{cases} \tag{2.10}$$

Also from the RH problem for $N(s)$, the constant c of the JT in (2.3) satisfies the equation

$$\frac{1}{2\pi i} \oint_\nu \frac{f(J_c(s))}{s} ds = 1 + \theta. \tag{2.11}$$

Thus the sum equation in the RH problem for $N(s)$ can be rewritten as,

$$(1-\gamma)(N_+(s_1) + N_-(s_2)) + 2\gamma f(J_c(s)) = 2V'(J_c(s))J_c(s). \tag{2.12}$$

Defining the inverse mapping of JT as,

$$s = J_c^{-1}(x) = h(x). \tag{2.13}$$

with $(s_1)_+ = h(y)$; $(s_2)_- = \bar{h}(y)$; $s_1 = h(x)$ and $s_2 = \bar{h}(x)$, we substitute for $[N_+(s_1) + N_-(s_2)]$ using equation (2.10) and the inverse mapping. We finally get the integral equation,

$$f(y;\gamma) = \frac{V'(y)y}{\gamma} - \frac{1-\gamma}{\gamma} \left[1 + \frac{1}{2\pi} \int_0^b f(x;\gamma)\phi(x,y)dx \right], \tag{2.14}$$

where

$$\phi(x,y) = \text{Im} \left[\left(\frac{1}{h(y) - \bar{h}(x)} + \frac{1}{\bar{h}(y) - \bar{h}(x)} \right) \bar{h}'(x) \right]. \tag{2.15}$$

We solve (2.14) for $f(y;\gamma)$ and (2.11) for c numerically, self-consistently. The new effective potential $V_{\text{eff}}(x;\gamma)$ is related to $f(x;\gamma)$ by

$$V'_{\text{eff}}(x;\gamma) = \frac{f(x;\gamma)}{x}. \tag{2.16}$$

The eigenvalue density for this effective potential is given by [1],

$$\sigma(y;\gamma) = \frac{-1}{2\pi^2 \gamma y} \int_b^0 x V'_{\text{eff}}(x;\gamma)\chi(x,y)dx,$$
$$\chi(x,y) = \text{Re} \left[\left(\frac{1}{\bar{h}(y) - h(x)} - \frac{1}{h(y) - h(x)} \right) h'(x) \right]. \tag{2.17}$$

III. EIGENVALUE DENSITY FOR β ENSEMBLES

In equation (1.1) if we take limit $\theta \to 1$ and $V(x) = \frac{\beta}{2}x$, we get jpd of Laguerre β ensembles with $\beta = 1+\gamma$. So in the analysis of Section II, if we take $\theta \to 1$ and $V(x) = \frac{\beta}{2}x$, we can compute eigenvalue density for Laguerre β ensembles for any $\beta > 1$. Note that equations (2.14)–(2.17) are valid only for $\theta > 1$. Thus we choose $\theta = 1.0001$ for the $\theta \to 1$ limit. In section IV C we analytically solve the RH problem explicitly for $\theta = 1$ case and show that the results are consistent with numerical solution for $\theta \to 1$. As $\theta \to 1$ the shape of contour ν approaches a circle. Figure 2 shows contour ν and its mapping for $\theta \to 1, c \to 0.5$.

Once the contour and the mapping (and consequently the inverse mapping) is known, we solve equation (2.11) and equation (2.14) self-consistently to find $f(x;\beta)$. Then the effective potential and the eigenvalue density are computed with equation (2.16) and equation (2.17), respectively, for $\beta = 1 + \gamma$.

IV. RESULTS

For the γ-ensembles, we first choose θ very close to 1 ($\theta = 1.0001$) and a linear external potential, $V(x) = 2x$.
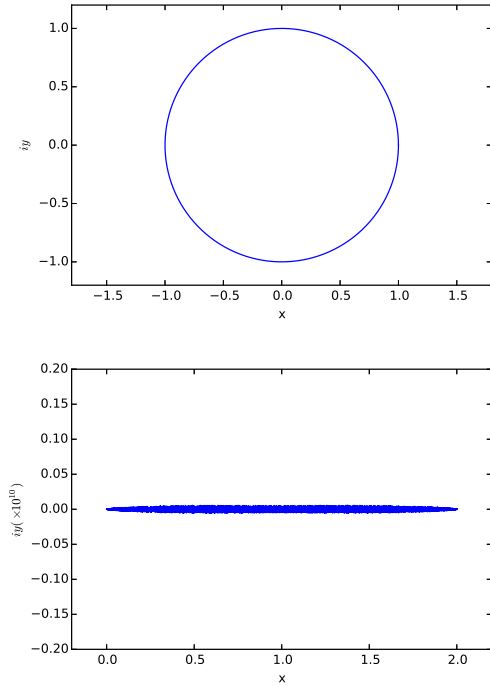
FIG. 2: (Color online) Top panel: ν contour for $\theta \to 1$, $c \to 0.5$. Bottom panel: mapping for $\theta \to 1$, $c \to 0.5$ (small scatter is due to numerical errors).

FIG. 3: (Color online) Effective potential near origin for different γ, $V(x) = 2x$ and $\theta = 1.0001$.

A. Effective potential near origin for $\theta = 1.0001$ ($\theta \to 1$ limit)

For $\theta = 1.0001$ and $V(x) = 2x$, after finding a self-consistent solution to $f(x; \gamma)$ using equation (2.14) and equation (2.11), we compute the effective potential using equation (2.16). The effective potential shows a qualitative change in its behavior near origin going from $\gamma < 1$ (or $\beta < 2$) to $\gamma > 1$ (or $\beta > 2$). Figure 3 shows that the effective potential is monotonically increasing for $\gamma > 1$. In contrast for $\gamma < 1$ the effective potential develops a minima and shows decreasing behavior near origin. The minima of effective potential moves further away from origin as γ decreases from 1. It has been shown in [7] that such a minima in confining potential, if deep enough, can produce transition from diverging eigenvalue density at hard-edge to non-diverging density. The γ-ensemble was originally considered as a solvable toy model for 3D disordered systems [1] whose eigenvalues x_i determine the conductance of the system. The parameter γ decreases from 1 as the strength of disorder increases. Taking $\theta = 1.0001$ in this toy model, we show here that for $\gamma < 1$ the corresponding effective potential deviates from the monotonically increasing behavior and has a minima which moves away from origin as γ is decreased. This minima is very close to the origin and is not sufficiently deep to produce the transition in density, as shown in Figure 7. However, the position and strength of the minima will depend on the competition between the nature of the additional interaction as well as the external confining potential. To show the effect of the confining potential, we consider a γ-ensemble with quadratic external potential $V(x) = \alpha x^2$, $\gamma = 0.7$ and $\theta \to 1$. We choose $\alpha = 0.2$ so that the potential is much weaker near the origin compared to the linear potential. Figure 4 shows that the minima of the effective potential is shifted significantly away from the origin and is deeper compared to the effective potentials in Figure 3.

We vary the exponent γ over a range of values to see how the effective potential and the eigenvalue density changes. The corresponding effective potential shows transition to a non-monotonic behavior as γ is changed from greater than 1 to less than 1. Such a nonmonotonic effective potential has been shown [7] to produce transition from a diverging to a non-diverging eigenvalue density near the origin. Note that the γ-ensemble with $\theta \to 1$, $\gamma = 3$ and $V(x) = 2x$ is also equivalent to the Laguerre β-ensemble with $\beta = 4$. The numerically computed eigenvalue density is compared with analytical result available for $\beta = 4$. From Section II and Section III we show that this eigenvalue density can be numerically computed for any $\beta \geq 1$. The analytical results for Laguerre beta ensembles obtained in Section IV C also suggest that the non-monotonicity of the effective potential should disappear at $\theta = 1$. To see this change in non-monotonic behavior we vary the value of θ near 1 for two representative values of $\gamma < 1$ ($\gamma = 0.6$) and $\gamma > 1$ ($\gamma = 3$). For $\gamma = 3$, we observe a transition from non-monotonic to monotonic effective potential as θ is varied and then the effective potential approaches a linear behavior as $\theta \to 1$. Similarly, effective potential for $\gamma = 0.6$ shows gradual decrease in non-monotonicity as $\theta \to 1$.
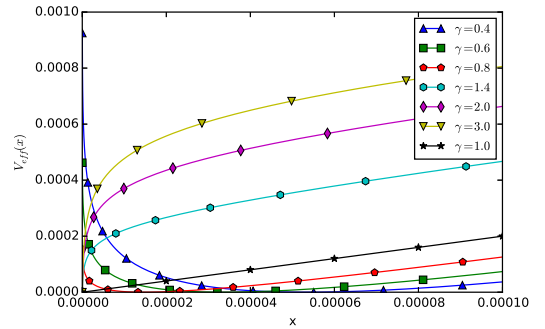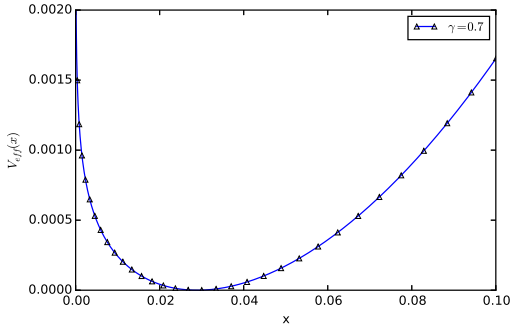
FIG. 4: (Color online) Effective potential near origin for quadratic potential $V(x) = 0.2x^2$, $\gamma = 0.7$ and $\theta = 1.0001$.

FIG. 5: (Color online) Effective potential for different β and $V(x) = 2x$.

B. Eigenvalue density for Laguerre β ensembles

For the eigenvalue density of Laguerre β ensembles with $\beta = 4$, we choose $V(x) = 2x$, $\theta = 1.0001$ and $\gamma = 3$. Solving for $f(x;\gamma)$ self-consistently using equation (2.14) and equation (2.11), we compute the corresponding eigenvalue density using equation (2.17). The numerical density matches very closely with the analytic result except near the soft edge where it underestimates the support slightly (see Figure 6). This is may be due to the fact that θ is not exactly equal to 1 and the small non monotonic behavior of $V_{\text{eff}}(x)$ near origin restricts the support to a slightly smaller value. Since the γ-ensemble formalism is valid for any $\gamma > 0$ and well behaved potential $V(x)$, we can numerically compute the eigenvalue density for any $\beta > 1$. Such an eigenvalue density is expected to be the same for all β [16]. Instead, we systematically change β (or γ) but keep the external potential same as $V(x) = 2x$. Though these are not classical β ensembles, the eigenvalue density obtained can be converted to Laguerre β ensemble density by appropriate scaling. We have already shown in Figure 3 an interesting qualitative behavior of these effective potentials near origin. In Figure 5 we show the effective potentials over the full support of density. The effective potential becomes less and less converging as β increases from 1.4 to 4 (or γ increases from 0.4 to 3). Figure 7 shows the densities calculated from equation (2.17) for different values of β. These numerical results also agree very well with the analytical expression (see equation (4.1)) for density obtained after appropriate scaling of equation (1.4) for $V(x) = 2x$ instead of $V(x) = \frac{\beta}{2}x$.

$$\sigma(x) = \begin{cases} \frac{2}{\pi}\frac{1}{\beta}(\frac{\beta-x}{x})^{\frac{1}{2}}, & \text{for } 0 < x < \beta, \\ \frac{2}{\pi}\beta^{-\frac{1}{2}}x^{-\frac{1}{2}}, & \text{for } x \to 0, \\ 0, & \text{for } x \geq \beta. \end{cases} \qquad (4.1)$$

All of the densities diverge near the hard-edge and the support of densities increases as β increases (see Figure 7). The numerical densities near origin when fitted to
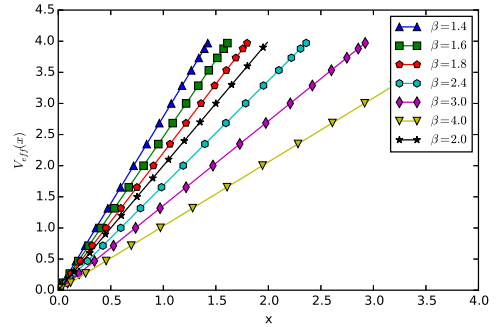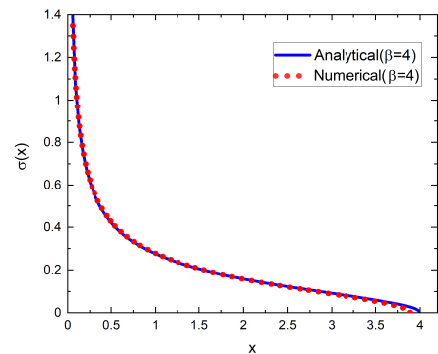

FIG. 6: (Color online) density for $\beta = 4$. The dotted line shows numerical result compared to analytical result shown with bold line.

curve $\sigma(x;\beta) = ax^b$ show that the exponents b are all $-\frac{1}{2}$ for different β. Figure 8 shows the prefactors a as function of β.

C. RH problem for $\theta = 1$

In this subsection we derive the analytic form of the effective potential for Laguerre β ensemble by exactly solving the RH problem for $\theta = 1$, $\gamma > 0$. The external potential for Laguerre β ensemble is $V(x) = \frac{\beta}{2}x = \frac{1+\gamma}{2}x$. For $\theta = 1$, contour ν is a unit circle in complex plane centered at origin. The regions inside and outside the contour ν are both mapped onto the same complex region $\mathbb{C}\backslash[0,b]$. Every point on the contour is mapped onto a point on real line in $[0,b]$. Schematic Figure 9 shows the mapping.

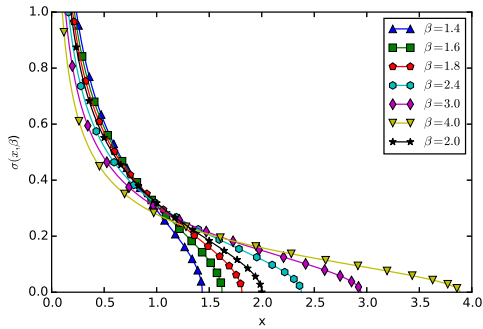When $\theta = 1$, equation (2.5) gives $g(z) = \tilde{g}(z)$. $M(s)$ is

FIG. 7: (Color online) Densities for different β and $V(x) = 2x$.

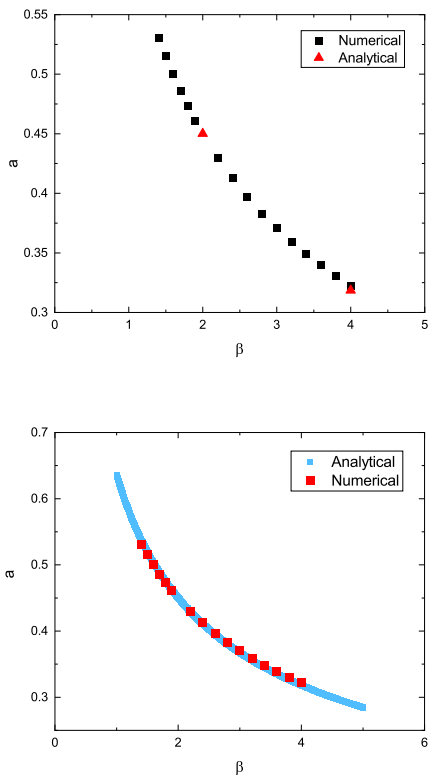
FIG. 8: (Color online) Densities near the origin are fitted to function $\sigma(x;\beta) = ax^b$. The graph shows prefactors a for different β. Top panel: Analytical result for $\beta = 2$ from equation (1.35) in [7] and for $\beta = 4$ from equation (1.4). Bottom panel: Analytical result from equation (4.1).

then defined as

$$M(s) \equiv \begin{cases} G(J_c(s)), & \text{for } s \in \mathbb{C}\backslash\bar{D}, \\ G(J_c(s)), & \text{for } s \in D\backslash[-1,0]. \end{cases} \quad (4.2)$$

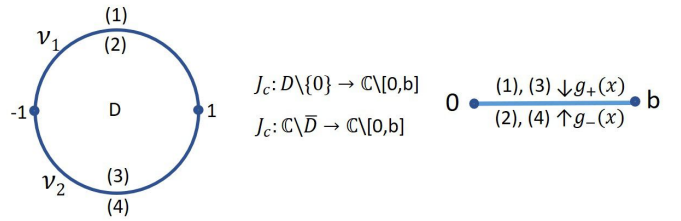Now since $\tilde{g}_+(x) = g_+(x)$, region (1) and region (3) in

FIG. 9: (Color online) Schematic figure for the mapping of JT for $\theta = 1$

the schematic mapping are one and the same. Similarly $\tilde{g}_-(x) = g_-(x)$ means region (2) and region (4) are same. In terms of functions $M(s)$ these relations can be written as $M_+(s_1) = M_+(s_2)$ and $M_-(s_1) = M_-(s_2)$ (see Figure 1). With $N(s) \equiv M(s)J_c(s)$, equation (2.8) now becomes

$$(1+\gamma)(N_+(s_1) + N_-(s_1)) = 2V'(J_c(s))J_c(s), \quad (4.3)$$

where $J_c(s) = J_c(s_1) = J_c(s_2) = x \in [0,b]$. With $f(J_c(s))$ defined according to equation (2.9) and $V(x) = \frac{\beta}{2}x = \frac{1+\gamma}{2}x$ for Laguerre β ensembles, we finally get,

$$\begin{aligned} f(x) &= x, \\ V_{\text{eff}}(x) &= x. \end{aligned} \quad (4.4)$$

Note that this result is also apparent from equation (1.4) which says that eigenvalue density for all Laguerre β ensembles is same and the fact that interaction term in MB ensemble at $\theta = 1$ is equivalent to that of Lagurre β ensembles for $\beta = 2$. Equation (4.4) tells us that the non-monotonicity of effective potentials previously shown for $\gamma < 1$ should disappear when $\theta = 1$. Figure (10) shows the effective potentials near the origin for $\gamma = 0.6$ and a range of values for θ between 1 and 2. We have shown in [1] that the effective potential for $\theta = 2$ monotonically goes to zero at the origin. As θ is reduced from 2, the effective potential develops a non-monotonicity. The minima of the effective potential gradually becomes deeper and moves away from the origin. Later as θ moves closer to 1, the depth of the minima of the effective potential decreases and the minima shifts closer to the origin. Thus with decreasing non-monotonicity, we expect the effective potential to become linear for $\theta = 1$ as predicted by equation (4.4). We also explore the change in the effective potential for $\gamma = 3$ for different values of θ near 1 (see Figure 11). Interestingly, the effective potential shows change from a non-monotonic to monotonic behavior near the origin at some intermediate value of θ before finally tending to linear behavior as $\theta \to 1$. Although within our numerical accuracy the effective potential near the origin does not always decrease consistently as θ is decreased, the general behavior tends towards the expected linear dependence, $V_{\text{eff}}(x) = x$, as $\theta \to 1$.

In the RH problem for $\theta = 1$, if we choose $V(x) = 2x$ instead of $\frac{\beta}{2}x$, equation(4.3) gives $f(x) = V_{\text{eff}}(x) = $
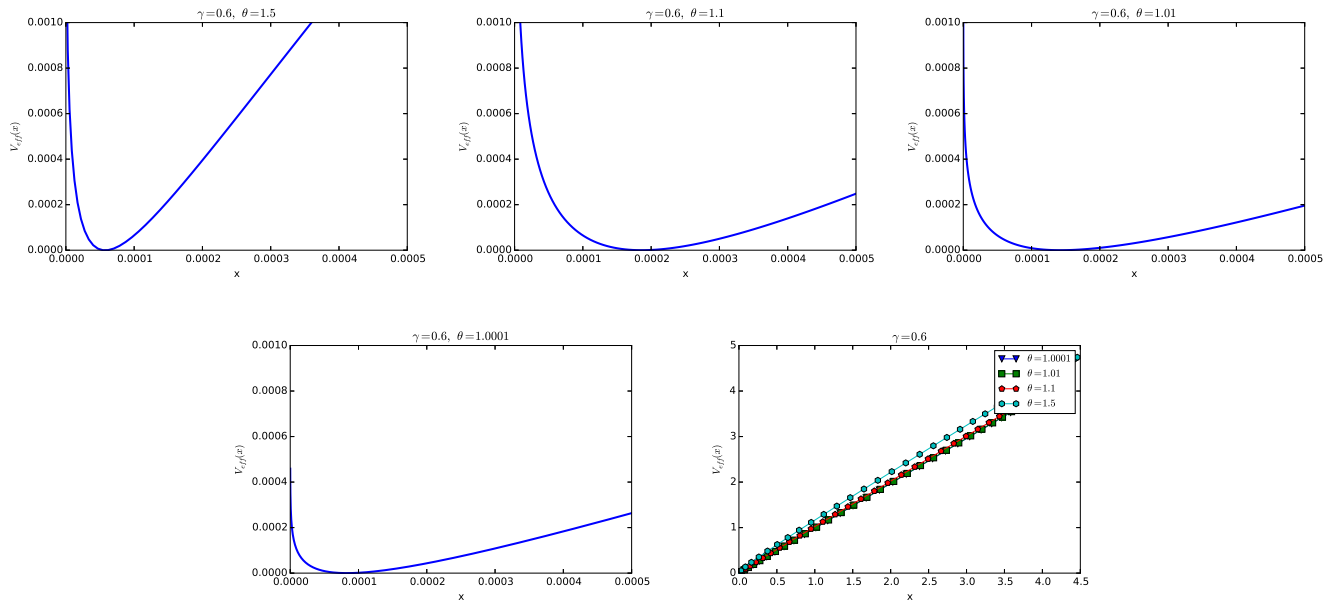
FIG. 10: (Color online) The effective potentials close to the origin and over the full support, for $\gamma = 0.6$ and different values of θ. Near the origin, the minima of the non-monotonic effective potential first moves away from the origin and then moves towards the origin as θ is reduced. We know from [1] that the effective potential is monotonic for $\theta = 2$. Also, consistent with the analytical result for $\theta = 1$, the non-monotonicity of effective potential near the origin reduces as $\theta \to 1$.
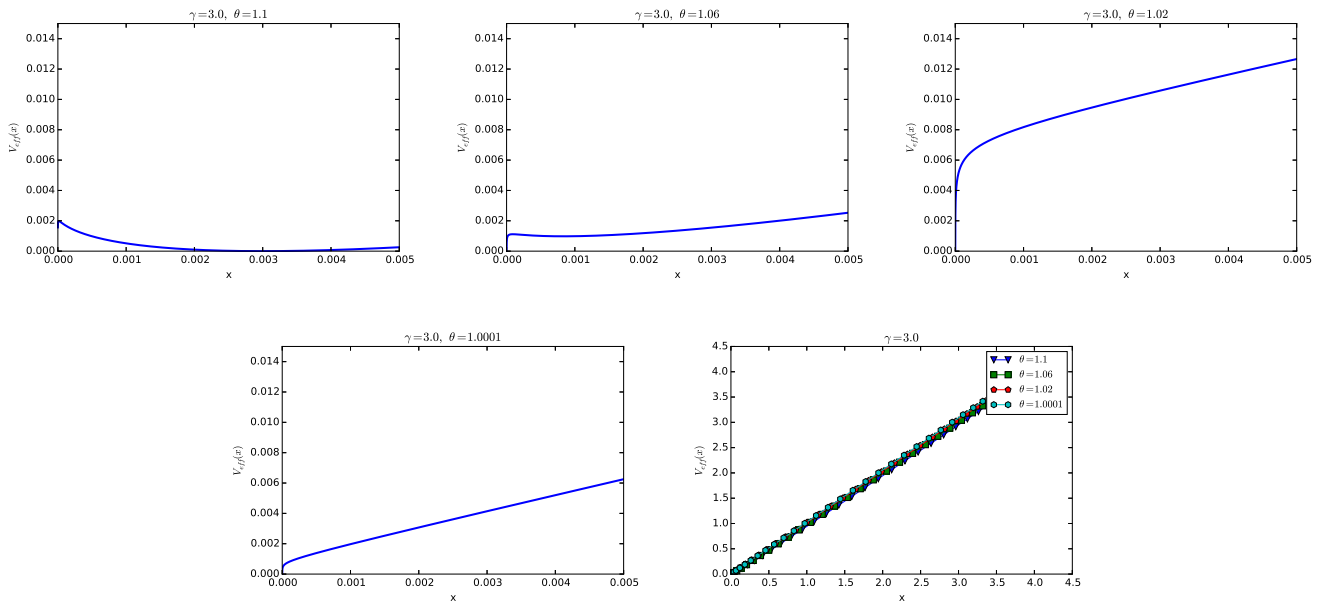

FIG. 11: (Color online) The effective potentials close to the origin and over the full support, for $\gamma = 3.0$ and different values of θ. It shows transition from a non-monotonic to a monotonic behavior of the effective potential near the origin for different values of θ. The effective potential tends to a linear behavior as predicted by the analytical result for $\theta = 1$.

$\frac{4}{1+\gamma}x$. The numerical results obtained for effective potential of γ ensemble with $\theta = 1.0001$ and $V(x) = 2x$ agree very well with this analytic expression (see Figure 5).

V. SUMMARY AND CONCLUSION

The eigenvalue density of γ-ensembles has previously been computed by solving the corresponding Riemann-Hilbert problem. We use the same method for different

values of θ close to 1 and $\gamma > 0$, and find that the effective potential becomes non-monotonic near the origin for $\gamma < 1$. The minimum of the effective potential shifts further away from the origin as γ is decreased systematically. While the shift and the depth of the minimum is not sufficient to produce a hard-edge to soft-edge transition in density in this toy model, it suggests that with appropriate combination of the additional interaction and the confining potential, such a transition can indeed occur. The exponent γ induced hard-edge to soft-edge transition in density describes disorder induced metal to insulator transition in mesoscopic systems. It would be interesting to see if (1.2) remains a good candidate for such a transition.

The limit $\theta \to 1$ corresponds to the Laguerre β-ensembles. This allows us to use the model to numerically compute the eigenvalue density for Laguerre β-ensembles for all $\beta > 1$. The results agree with various expected analytical expressions including the ones from the exact analytical solution to RH problem for $\theta = 1$. This shows the applicability of the effective potential method for general γ-ensembles with different values of $\theta > 1$ and $\gamma > 0$.

VI. ACKNOWLEDGMENT

References

[1] Yadav S, Alam K, Muttalib K A and Wang D 2020 *J. Phys. A* **53** 015001, 15 ISSN 1751-8113 URL https://doi.org/10.1088/1751-8121/ab56e0

[2] Muttalib K A 1995 *J. Phys. A* **28** L159–L164 ISSN 0305-4470 URL http://stacks.iop.org/0305-4470/28/L159

[3] Borodin A 1999 *Nuclear Phys. B* **536** 704–732 ISSN 0550-3213 URL http://dx.doi.org/10.1016/S0550-3213(98)00642-7

[4] Forrester P J and Wang D 2017 *Electron. J. Probab.* **22** Paper No. 54, 43 ISSN 1083-6489 URL https://doi.org/10.1214/17-EJP62

[5] Zhang L 2015 *J. Stat. Phys.* **161** 688–711 ISSN 0022-4715 URL http://dx.doi.org/10.1007/s10955-015-1353-3

[6] Kuijlaars A B J and Molag L D 2019 *Nonlinearity* **32** 3023–3081 ISSN 0951-7715 URL https://doi.org/10.1088/1361-6544/ab247c

[7] Claeys T and Romano S 2014 *Nonlinearity* **27** 2419–2444 ISSN 0951-7715 URL http://dx.doi.org/10.1088/0951-7715/27/10/2419

[8] Muttalib K A, Pichard J L and Stone A D 1987 *Phys. Rev. Lett.* **59**(21) 2475–2478 URL https://link.aps.org/doi/10.1103/PhysRevLett.59.2475

[9] Muttalib K A and Klauder J R 1999 *Phys. Rev. Lett.* **82**(21) 4272–4275 URL https://link.aps.org/doi/10.1103/PhysRevLett.82.4272

[10] Muttalib K A and Gopar V A 2002 *Phys. Rev. B* **66**(11) 115318 URL https://link.aps.org/doi/10.1103/PhysRevB.66.115318

[11] Douglas A, Markoš P and Muttalib K A 2014 *J. Phys. A* **47** 125103, 13 ISSN 1751-8113 URL https://doi.org/10.1088/1751-8113/47/12/125103

[12] Muttalib K A, Markoš P and Wölfle P 2005 *Phys. Rev. B* **72**(12) 125317 URL https://link.aps.org/doi/10.1103/PhysRevB.72.125317

[13] Forrester P J 1994 *J. Math. Phys.* **35** 2539–2551 ISSN 0022-2488 URL https://doi.org/10.1063/1.530883

[14] Baker T H and Forrester P J 1997 *Comm. Math. Phys.* **188** 175–216 ISSN 0010-3616 URL https://doi.org/10.1007/s002200050161

[15] Johansson K 1998 *Duke Math. J.* **91** 151–204 ISSN 0012-7094 URL https://doi.org/10.1215/S0012-7094-98-09108-6

[16] Forrester P J 1993 *Nuclear Phys. B* **402** 709–728 ISSN 0550-3213 URL https://doi.org/10.1016/0550-3213(93)90126-A